

See discussions, stats, and author profiles for this publication at: <https://www.researchgate.net/publication/320355590>

# A filamentous bacteriophage targeted to carcinoembryonic antigen induces tumor regression in mouse models of colorectal cancer

Article in *Cancer Immunology and Immunotherapy* · October 2017

DOI: 10.1007/s00262-017-2076-x

CITATIONS

5

READS

134

12 authors, including:



**Paola Murgas**

Universidad Mayor

9 PUBLICATIONS 95 CITATIONS

[SEE PROFILE](#)



**Eduardo Duran**

University of Desarrollo

3 PUBLICATIONS 5 CITATIONS

[SEE PROFILE](#)



**Diana Gaete**

Universitätsklinikum Carl Gustav Carus Dresden

4 PUBLICATIONS 6 CITATIONS

[SEE PROFILE](#)



**César Oyarce**

Fundación Ciencia Para la Vida

10 PUBLICATIONS 109 CITATIONS

[SEE PROFILE](#)

Some of the authors of this publication are also working on these related projects:




Bacteriophage immunotherapy against gastrointestinal cancers [View project](#)



Exosomes and breast cancer [View project](#)

# A filamentous bacteriophage targeted to carcinoembryonic antigen induces tumor regression in mouse models of colorectal cancer

Paola Murgas<sup>1</sup> · Nicolás Bustamante<sup>1</sup> · Nicole Araya<sup>1</sup> · Sebastián Cruz-Gómez<sup>1</sup> · Eduardo Durán<sup>1</sup> · Diana Gaete<sup>1</sup> · César Oyarce<sup>1</sup> · Ernesto López<sup>1</sup> · Andrés Alonso Herrada<sup>1</sup> · Nicolás Ferreira<sup>2</sup> · Hans Pieringer<sup>2</sup> · Alvaro Lladser<sup>1</sup> 

Received: 22 November 2016 / Accepted: 3 October 2017  
© Springer-Verlag GmbH Germany 2017

**Abstract** Colorectal cancer is a deadly disease, which is frequently diagnosed at advanced stages, where conventional treatments are no longer effective. Cancer immunotherapy has emerged as a new form to treat different malignancies by turning-on the immune system against tumors. However, tumors are able to evade antitumor immune responses by promoting an immunosuppressive microenvironment. Single-stranded DNA containing M13 bacteriophages are highly immunogenic and can be specifically targeted to the surface of tumor cells to trigger inflammation and infiltration of activated innate immune cells, overcoming tumor-associated immunosuppression and promoting antitumor immunity. Carcinoembryonic antigen (CEA) is highly expressed in colorectal cancers and has been shown to promote several malignant features of colorectal cancer cells. In this work, we targeted M13 bacteriophage to CEA, a tumor-associated antigen over-expressed in a high proportion of colorectal cancers but largely absent in normal cells. The CEA-targeted M13 bacteriophage was shown to specifically bind to purified CEA and CEA-expressing tumor cells *in vitro*. Both intratumoral and systemic administration of CEA-specific bacteriophages significantly reduced tumor growth of mouse models of colorectal cancer, as compared to PBS and control bacteriophage administration. CEA-specific bacteriophages promoted tumor infiltration of neutrophils and macrophages, as well as maturation dendritic cells in tumor-draining lymph nodes, suggesting that antitumor T-cell responses were

elicited. Finally, we demonstrated that tumor protection provided by CEA-specific bacteriophage particles is mediated by CD8<sup>+</sup> T cells, as depletion of circulating CD8<sup>+</sup> T cells completely abrogated antitumor protection. In summary, we demonstrated that CEA-specific M13 bacteriophages represent a potential immunotherapy against colorectal cancer.

**Keywords** Colorectal cancer · Bacteriophages · Carcinoembryonic antigen · Cancer immunotherapy

## Abbreviations

αCEA	Carcinoembryonic antigen-specific
CEA	Carcinoembryonic antigen
CRC	Colorectal cancer
TAM	Tumor-associated macrophages
TAN	Tumor-associated neutrophils
WT	Wild-type

## Introduction

Colorectal cancer (CRC) is a leading cause of death in developed countries [1]. CRC is frequently diagnosed at advanced stages of the disease, at which risk of recurrence is high despite an initial successful surgery and adjuvant chemotherapy [2, 3]. Moreover, patients with advanced CRC show poor response to conventional chemotherapeutic treatments, such as 5-fluorouracil [4, 5]. Therefore, novel approaches are needed to effectively treat patients with CRC. Cancer immunotherapy has emerged as a new form to treat different malignancies by boosting the ability of the immune system to control tumor growth and fight cancer [6–9]. CD8 T cells play a pivotal role in specifically recognizing tumor cells and eliminating them by cytotoxic mechanisms [10, 11]. In addition, cytotoxic CD8 T cells orchestrate other arms

✉ Alvaro Lladser  
alladser@cienciavida.org

<sup>1</sup> Laboratory of Gene Immunotherapy, Fundación Ciencia & Vida, Av. Zañartu 1482, Ñuñoa, 7780272 Santiago, Chile

<sup>2</sup> Phage Technologies, Parque Tecnológico Zañartu, Av. Zañartu 1482, Ñuñoa, 7780272 Santiago, Chile

of the innate immune responses with antitumor potential such as neutrophils and macrophages. However, despite the generation of endogenous antitumor T-cell responses early in tumor development, clinically relevant tumors are able to suppress antitumor immune responses by a plethora of mechanisms, including the generation of an immunosuppressive microenvironment that reprograms myeloid cells to a pro-tumoral phenotype and renders CD8 T cell dysfunctional and/or hyporesponsive [12–16]. Hence, strategies overcoming tumor-induced immunosuppressive microenvironment may achieve effective antitumor immune responses and protection against CRC.

M13 bacteriophage is a highly immunogenic agent containing single-stranded DNA, which is a potent stimulator of several DNA-sensing innate immune receptors [17]. Bacteriophages have been used for antigen delivery and demonstrated to activate innate immunity and consequently trigger both humoral and cellular immune responses in the absence of other adjuvants [18–22]. Bacteriophage immunogenicity relies on their ability to activate DNA-sensing innate immune receptors, such as TLR9, and the downstream MyD88-dependent signaling pathways [21, 22]. The ability of bacteriophages to activate innate immune cells and promote a pro-inflammatory milieu also has been used to overcome the tumor-induced immunosuppressive microenvironment [23, 24]. Bacteriophages can be specifically targeted via single chain variable fragments (scFv) derived from a monoclonal antibody to antigens expressed at the surface of tumor cells [23–25]. Tumor cell-associated bacteriophages promote acute inflammation and recruitment of activated innate immune cells by MyD88-dependent mechanisms, leading to tumor regression in a model of melanoma [24]. In that study, melanoma-targeted bacteriophages induce the infiltration of neutrophils and macrophages, the latter switching from a M2- to a M1-polarized phenotype [24]. Interestingly, bacteriophage administration increased the expression of costimulatory receptors and molecules involved in antigen presentation, suggesting that antitumor T-cell responses may be promoted by this strategy, although no direct evidence demonstrating the generation of bacteriophage-induced tumor-specific T-cell responses has been reported. M13 bacteriophage-associated antitumor activity was shown to be dependent on MyD88-dependent signaling pathways, which is downstream of the activation of innate immune receptors, including DNA-sensing TLR9. Indeed, no signs of tumor destruction or neutrophil infiltration were observed in MyD88<sup>-/-</sup> mice treated with tumor-specific scFv-targeted bacteriophages.

Carcinoembryonic antigen (CEA) is a membrane glycoprotein highly expressed in CRC, but largely absent in adult normal tissues [26, 27]. CEA is implicated in cell adhesion, cell-to-cell interactions and signal transduction [28]. Several reports implicate CEA in cancer progression and metastasis

[29–31]. Recently, Bajenova and coworkers compared the genome-wide transcriptomic profiles of CEA-positive and CEA-negative colorectal cancer cell lines with different metastatic potential. Their results suggest that the expression of CEA favors cancer progression by inducing the epithelial-to-mesenchymal transition, increasing tumor cell invasiveness and suppressing stress and apoptotic signaling [32]. Moreover, high CEA serum levels are correlated with cancer progression [30], and autocrine pro-tumoral properties by inhibiting differentiation and apoptosis [33–35]. Hence, CEA is one of the most attractive antigens to be used for cancer immunotherapy [36]. In this work, we generated a CEA-specific ( $\alpha$ CEA) M13 bacteriophage able to associate with CEA-expressing tumor cells to promote tumor infiltration of neutrophils and macrophages, as well as maturation of dendritic cells in tumor-draining lymph nodes. Interestingly, CEA-specific bacteriophage suppressed tumor growth in mouse models of colorectal cancer through a CD8<sup>+</sup> T-cell-dependent mechanism.

## Materials and methods

### Production of M13 bacteriophages

The *E. coli* ER2738 was grown in Luria–Bertani (LB) medium with 20 mg/ml of tetracycline and infected with 10<sup>12</sup> pfu/ml of M13 filamentous bacteriophages for 4.5 h at 37 °C with constant shaking. For producing  $\alpha$ CEA M13 bacteriophages, a protocol described by Rondot et al. [37] was used. Briefly, *E. coli* ER2738 was transformed with pSEX81 plasmid (PROGEN) carrying the CEA-specific scFv inserted at NcoI and BamHI restriction sites upstream of the pIII protein coding sequence. These bacteria were infected for 15 h at 30 °C with a multiplicity of infection of 20 of hyperphage (PROGEN), which contains all genes of structural proteins of M13 bacteriophage (except for pIII protein). M13 bacteriophages present in bacteria culture supernatants were concentrated using 20% polyethylene glycol at 4 °C [38]. Elimination of LPS was performed by extraction with Triton X-114 (Sigma-Aldrich), as previously described [39]. Purified bacteriophages particles were tested for endotoxin contamination using the Limulus amoebocyte lysate assay (QCL-1000, Lonza) according to the manufacturer's instructions. Endotoxin levels were < 0.05 EU/ml in all bacteriophage preparations.

### Titration of M13 bacteriophages

ELISA 96-well plates (MaxiSorp, Nunc) were incubated with serial dilutions of  $\alpha$ CEA and WT M13 bacteriophages in 0.1 M sodium bicarbonate buffer (pH 8.2) for 16 h at 4 °C. Hyperphage dilutions with known concentrations were used

to generate a standard curve. Blocking was performed using phosphate-buffered saline (PBS) 5% bovine serum albumin (BSA). Bacteriophages and hyperphage were detected using an anti-pIII monoclonal antibody (clone A23, New England Biolabs) diluted 1:1000, followed by incubation with goat anti-mouse IgG secondary antibody coupled to horseradish peroxidase (HRP) (Thermo Fisher Scientific) diluted 1:5000 in PBS 0.1% Tween-20. Washing steps were performed with PBS 0.1% Tween-20. HRP activity was revealed by incubating with 1 mg/ml 3,3',5,5'-tetramethylbenzidine. The absorbance was measured at 630 nm in spectrophotometer (Synergy HT, BioTek).

### Western blot

The expression of scFv/pIII fusion protein or unmodified pIII protein was analyzed by sodium dodecyl sulfate polyacrylamide gel electrophoresis and Western blotting. Briefly, 12% polyacrylamide gel was loaded with equal amounts of  $\alpha$ CEA or WT M13 bacteriophages diluted in PBS. Then, proteins were transferred to a nitrocellulose membrane, which was blocked with 5% fat-free milk in PBS and was incubated with a monoclonal anti-pIII (clone A23, New England Biolabs) antibody diluted 1:1000 in PBS 5% fat-free milk overnight at 4 °C. Then, the nitrocellulose membrane was incubated with a HRP-coupled goat anti-mouse IgG secondary antibody (Thermo Fisher Scientific) 1:3000 and incubation for 4 h at room temperature. The visualization of the bands corresponding to pIII protein (~ 70 kDa) or fusion protein scFv-pIII (~ 100 kDa) was performed with the SuperSignal West Pico chemiluminescent substrate (Thermo Fisher Scientific).

### Assessing specificity of M13 bacteriophages

ELISA 96-well plates (MaxiSorp, Nunc) were incubated with 1  $\mu$ g/ml of human CEA protein (cat#30-AC32, Fitzgerald) diluted in 0.1 M sodium bicarbonate buffer (pH 8.2) for 16 h at 4 °C. Then, wells were blocked using PBS 5% BSA. Serial dilutions of  $\alpha$ CEA and M13 bacteriophages were incubated for 2 h at room temperature and washed three times with Tris-buffered saline (TBS) 0.1% Tween-20. Bound M13 bacteriophages were detected using a mouse monoclonal antibody against M13 major coat protein (27-9420-01, GE Healthcare), followed by three washing steps with Tris-buffered saline (TBS) 0.1% Tween-20. Then, wells were incubated with secondary HRP-coupled antibody (cat# 32230, Thermo Fisher Scientific) diluted 1:5000. HRP activity was revealed by incubating with 1 mg/ml chromogenic substrate 3,3',5,5'-tetramethylbenzidine. The absorbance was measured at 630 nm in a spectrophotometer (Synergy HT, BioTek). To evaluate specific binding of  $\alpha$ CEA bacteriophages to CEA-expressing tumor cells, murine colon

adenocarcinoma cell lines MC38, MC38-CEA, CT26 and CT26-CEA were collected and washed twice with PBS 2% FBS. Cells ( $2 \times 10^5$ ) were incubated with specific  $\alpha$ CEA and WT M13 bacteriophages ( $10^{11}$  pfu) for 1, 5 h at 4 °C diluted in PBS fat-free milk 2.5%. Then cells were washed three times with PBS 2% FBS and incubated with mouse monoclonal antibodies against M13 major coat protein (27-9420-01, mouse IgG2a, GE Healthcare) and CEA (clone CB30, mouse IgG1, Cell Signaling) diluted in PBS 2% FBS for 1 h at 4 °C. After three washes with PBS 2% FBS cell were incubated with rat antibodies against mouse IgG2a (clone RMG2a-62, Biolegend) and mouse IgG1 (clone RMG1-1, Biolegend) diluted 1:100 in PBS 2% FBS for 30 min at 4 °C. Cells were analyzed by flow cytometry using a FACSCanto II instrument.

### Cell lines and culture

All cell lines were grown in complete Roswell Park Memorial Institute Medium (RPMI) 1640 supplemented with 10% FBS, 100 U/ml ampicillin and 100 U/ml streptomycin. MC38 and MC38-CEA tumor cell line were kindly donated by Dr. Hinrich Abken (University of Cologne, Germany). CT26 (CRL-2638) and HEK293T (CRL-3216) cell lines were purchased from the American Type Culture Collection (ATCC). CT26 cells were transduced to stably express CEA protein. Briefly, HEK293T cells were transfected with plasmids pSV-G, p-d8.91 (donated from Dr. Manuel Varas, Universidad de los Andes) and pEZ-Lv201 CEACAM5 (purchased in Genecopoeia). The viral particles obtained from supernatant were used to transduce CT26 cells. The CEA-expressing CT26 cells were sorted using FACSARIA II equipment and cultured in complete RPMI medium with 10  $\mu$ g/ml puromycin.

### Mice and tumor models

BALB/c and C57BL/6 mice were purchased from Jackson Laboratories and maintained at the animal facility of Fundacion Ciencia & Vida according to the “guide to care and use of experimental animals, Canadian council on animal care”. This study was carried out in accordance with the recommendations of the “guidelines for the welfare and use of animals in cancer research, Committee of the National Cancer Research Institute”. The protocol was approved by the “Committee of Bioethics and Biosafety” from Fundacion Ciencia & Vida. Six- to eight-week-old mice were subcutaneously (s.c.) injected in the right flank with  $5 \times 10^5$  CT26-CEA cells (BALB/c background) or  $7 \times 10^5$  MC38-CEA cells (C57BL/6 background) in 100  $\mu$ l of sterile PBS. After 7–10 days, animals were randomly assigned to the treatment groups. Mice were intratumorally (i.t.) or intravenously (i.v.) injected once (MC38-CEA) or four times (CT26-CEA)

every 48 h with PBS or  $10^{11}$  pfu of either WT or  $\alpha$ CEA M13 bacteriophages in a volume of 100  $\mu$ l of PBS. Perpendicular tumor diameters were measured three times a week using a digital caliper and tumor volume calculated. Mice were killed when moribund or when the mean tumor diameter  $\geq 15$  mm, according to the approved ethical protocol. For re-challenge experiments, mice that survived to CT26-CEA challenge were injected subcutaneously with  $5 \times 10^5$  CT26-CEA cells in the left flank, 60 days after the first challenge. For tumor microenvironment studies, the animals with a palpable subcutaneous tumor were i.t. injected with a single dose of PBS,  $10^{11}$  pfu of M13 WT or  $\alpha$ CEA bacteriophages and killed 22–24 h later. Tumors, spleens, draining and non-draining lymph nodes were obtained to evaluate immune cells by flow cytometry analysis. For studies involving in vivo depletion of CD8 T cells, animals were challenged with CT26-CEA cells and 24 h later were intraperitoneally (i.p.) injected with 0.01 mg of an anti-CD8 antibody (clone YTS-169.4, BioXCell) or an isotype-matched control antibody (clone LTF-2, BioXCell) in 100  $\mu$ l of PBS three times every 24 h. Then, animals received three additional i.p. injections of depletion or isotype antibodies every 72 h.

### Flow cytometry

Tumors, lymph nodes and spleen were processed through mechanic disruption and enzymatic digestion using 0.25 mg/ml of DNase and 1 mg/ml of type IV collagenase for 30 min at 37 °C. All tissues were washed with PBS and then incubated with specific antibodies for detection of different immune cells. Monoclonal anti-mouse antibodies used for flow cytometry were all from Biolegend and were as follows: CD45.2 (clone 104), CD80 (clone 16-10A1), F4/80 (clone BM8), MHC-II (clone M5/114.15.2), Ly6G (clone 1A8), CD86 (clone GL-1), CD11b (clone N418), CD11c (clone N418), and CD86 (clone GL-1). Zombie Aqua fixable viability dye was used to discriminate live cells. Staining was performed in PBS 2% FBS for 30 min at 4 °C and washed twice with PBS 2% FBS. Finally, cells were fixed in 2% paraformaldehyde and analyzed using a BD FACSCanto II flow cytometer (Becton–Dickinson) and FlowJo software v10.0.8.

### Statistical analysis

Data are expressed as mean  $\pm$  SEM. Statistical analysis was performed using the Graphpad Prism v6 software (Graphpad Software Inc.). Analyses between experimental groups were performed using unpaired two-tailed Student's *t* test. To evaluate statistical differences among Kaplan–Meier survival curves, a Log-Rank (Mantel–Cox) test was performed. Differences were considered statistically significant when *p* values were  $< 0.05$ .

## Results

### Generation of $\alpha$ CEA M13 bacteriophages

To investigate the potential of M13 bacteriophages to be used as an immunotherapeutic strategy against CRC, we generated a CEA-specific ( $\alpha$ CEA) M13 bacteriophage by fusing pIII protein to a scFv obtained from a monoclonal antibody specific for CEA (clone SCA431). The DNA encoding the scFv derived from the SCA431 antibody was synthesized and inserted into pSEX81 plasmid (*phagemid*) upstream of the pIII coding sequence. The resulting construct pSEX81-scFv (SCA431) was used to transform *E. coli* ER2738 carrying the hyperphage plasmid, which encodes for all M13 bacteriophage genes, except for the gene encoding the pIII protein. This bacteriophage M13 scFv (SCA431), termed M13  $\alpha$ CEA, was obtained from transformed *E. coli* ER2738 cultures. The wild-type M13 bacteriophage (M13 WT) was obtained from M13KE plasmid-transformed *E. coli* ER2738 cultures. WT and  $\alpha$ CEA M13 bacteriophages were purified and then quantified by indirect ELISA using serial dilutions of commercially available M13 bacteriophage particles for standard curve. The correct generation of scFv/pIII fusion protein was demonstrated by SDS-PAGE and Western blot using a specific antibody against pIII protein (Fig. 1a). As expected, analysis of M13  $\alpha$ CEA showed a band of  $\sim 100$  kDa corresponding to the CEA-specific scFv fused to pIII protein (Fig. 1a, right lane). In contrast, M13 WT displayed a smaller size of  $\sim 70$  kDa, which corresponds to the native pIII protein (Fig. 1a, left lane). The ability of M13  $\alpha$ CEA to bind to its cognate antigen was evaluated in vitro by indirect ELISA using plates coated with CEA purified from human biopsies (Fig. 1b). We observed that WT M13 bacteriophages did not significantly associate to CEA- or control-coated plates. In contrast, M13  $\alpha$ CEA specifically bound to CEA (Fig. 1b). To further investigate whether M13  $\alpha$ CEA was able to bind to CEA present at the surface of tumor cells, we co-incubated bacteriophage particles with murine colon adenocarcinoma cancer cell lines CT26 and MC38, and the sub-lines that stably express CEA CT26-CEA and MC38-CEA, respectively. The presence of bacteriophages and CEA expression at the surface of tumor cells were evaluated by flow cytometry (Fig. 1c). As shown in Fig. 1c, M13  $\alpha$ CEA, but not M13 WT, specifically bound to CEA-expressing tumor cells. The association of M13  $\alpha$ CEA was dependent on CEA levels. As expected, neither M13  $\alpha$ CEA nor M13 WT associated to cells non-expressing CEA CT26 and MC38. These results indicate that M13  $\alpha$ CEA displays CEA-specific scFv-pIII fusion protein to specifically associate to purified CEA and CEA-expressing tumor cells.

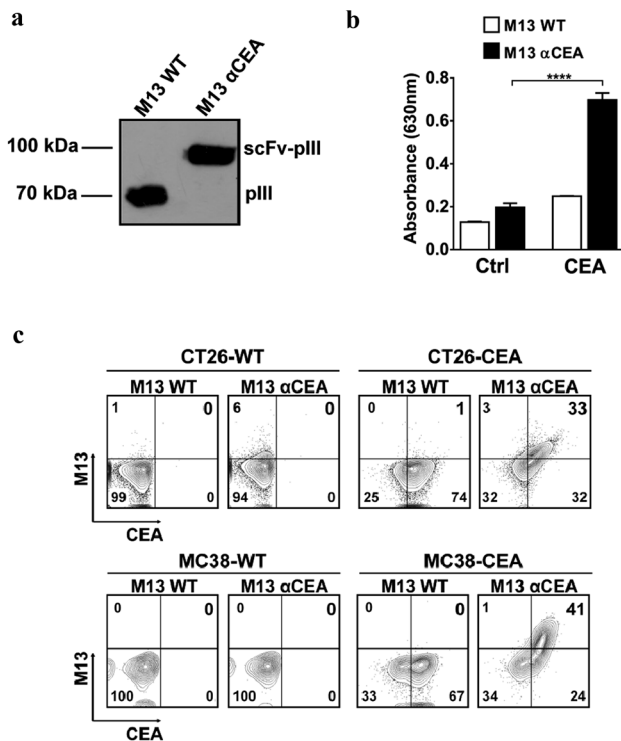


**Fig. 1** Characterization of  $\alpha$ CEA M13 bacteriophages. **a** The presence of native pIII or fused scFv/pIII proteins in WT and  $\alpha$ CEA M13 bacteriophages, respectively, was evaluated by Western blot using a monoclonal antibody specific against M13 pIII protein. **b** The ability of  $\alpha$ CEA M13 bacteriophage to bind to immobilized CEA protein was evaluated by ELISA. BSA-(Ctrl) and CEA-coated plates were incubated with either M13 WT or M13  $\alpha$ CEA bacteriophages, washed and then bound M13 bacteriophages were detected using an antibody against M13 major coat protein followed by a secondary HRP-coupled antibody and absorbance was measured at 630 nm. Data representative of at least two independent experiments is expressed as mean  $\pm$  SEM and statistical differences were analyzed by Student's *t* test. \*\*\*\**p* < 0.0001. **c** The expression of CEA and the association of WT M13 and  $\alpha$ CEA M13 bacteriophages to mouse colon cancer cell lines CT26, CT26-CEA (upper panels), MC38 and MC38-CEA (lower panels) was evaluated by flow cytometry using monoclonal antibodies against CEA and M13 major coat protein. Representative contour plots showing the relative percentage of each quadrant are shown for each condition. Data shown are representative of at least two independent experiments

### Intratumoral and systemic administration of $\alpha$ CEA M13 bacteriophages reduced the growth of CEA-expressing tumors in mouse models of colorectal cancer

To evaluate the ability of M13  $\alpha$ CEA to suppress the growth of a highly aggressive and fast growing CRC model, BALB/c mice carrying palpable s.c. CT26-CEA tumors ( $\sim 10 \text{ mm}^3$ —day 7) received four intratumoral administrations ( $1 \times 10^{11}$  pfu) 2 days apart of either M13 WT or M13  $\alpha$ CEA. Tumor-bearing mice injected with a saline solution (PBS) were used as a control group, which rapidly (within

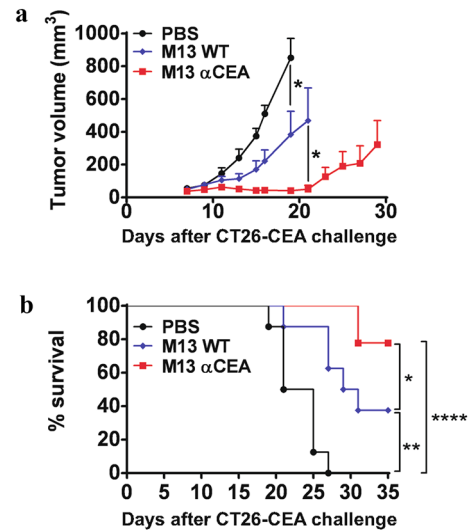


**Fig. 2** Growth of CT26-CEA tumors and survival of mice treated with M13 bacteriophages. BALB/c mice were subcutaneously injected with CT26-CEA tumor cells and 7 days later, mice bearing palpable tumors were intratumorally injected with four doses every 2 days of PBS, or  $1 \times 10^{11}$  pfu of either M13 WT or M13  $\alpha$ CEA bacteriophages. Tumor growth (**a**) and survival curves (**b**) for groups treated with PBS (circles), M13 WT (diamonds), M13  $\alpha$ CEA (squares) are shown. Representative data of at least two independent experiments using 8–9 mice per group are shown. The mean  $\pm$  SEM are shown. Survival curves were analyzed by Log-rank (Mantel–Cox) test. \**p* < 0.05; \*\**p* < 0.005; \*\*\*\**p* < 0.0001

3–4 weeks) succumbed to CT26-CEA tumors (Fig. 2a). M13  $\alpha$ CEA bacteriophage administration significantly reduced the growth of CT26-CEA tumors as compared to PBS and M13 WT groups (Fig. 2a). In addition, M13  $\alpha$ CEA administration greatly extended mouse survival, and  $\sim 75\%$  of mice completely rejected tumors (Fig. 2b). Although weaker, M13 WT administration also had a significant antitumor effect, determined as reduced tumor growth (Fig. 2a) and extended mouse survival (Fig. 2b). To test the antitumor potential of M13  $\alpha$ CEA in a more immunogenic and slowly growing tumor model, we challenge C57BL/6 mice with MC38-CEA cells and 7 days later, palpable tumors were injected with one dose of PBS, M13 WT or M13  $\alpha$ CEA. In this model, control mice started reaching maximal tumor size not earlier than 6 weeks after challenge. Administration of M13  $\alpha$ CEA significantly reduced the growth of MC38-CEA tumors (Fig. 3a) and extended mice survival (Fig. 3b) as compared to control group (PBS). M13 WT showed an intermediate effect that was not statistically significant, probably due to higher data dispersion of this model as compared to the CT26-CEA model. Then, to test whether M13  $\alpha$ CEA bacteriophage administered systemically would also impact tumor growth, mice bearing subcutaneous CT26-CEA tumors were intravenously injected with PBS, M13 WT or M13  $\alpha$ CEA. Remarkably, systemic administration of

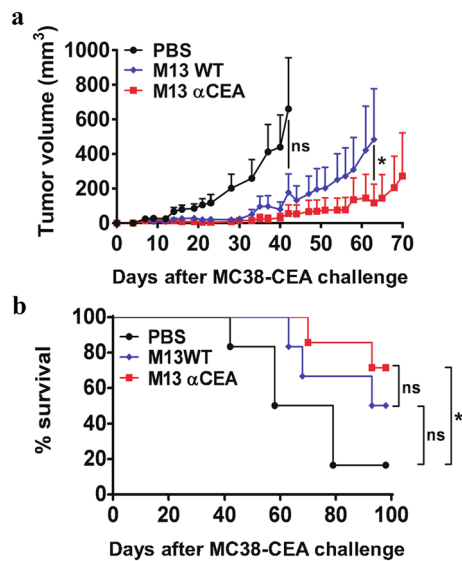


**Fig. 3** Growth of MC38-CEA tumors and survival of mice treated with M13 bacteriophages. C57BL/6 mice were subcutaneously injected with MC38-CEA tumor cells and 7 days later, mice bearing palpable tumors were intratumorally injected with one dose of PBS, or  $1 \times 10^{11}$  pfu of either M13 WT or M13  $\alpha$ CEA bacteriophages. Tumor growth (a) and survival curves (b) for groups treated with PBS (circles), M13 WT (diamonds), M13  $\alpha$ CEA (squares) are shown. Representative data of at least two independent experiments using 6–7 mice per treatment group are shown. The mean  $\pm$  SEM are shown. Survival curves were analyzed by Log-rank (Mantel–Cox) test. \* $p < 0.05$ ; ns non-significant

M13  $\alpha$ CEA efficiently suppressed the growth of CT26-CEA tumors (Fig. 4a) and extended mouse survival (Fig. 4b), as compared to PBS- and M13 WT-treated mice. These results lead us to conclude that M13  $\alpha$ CEA efficiently suppress the growth of CEA-expressing tumors in mouse models of colorectal cancer.

#### Intratumoral administration of $\alpha$ CEA M13 bacteriophages promotes tumor infiltration of myeloid cells and maturation of dendritic cells in secondary lymphoid organs

To investigate the mechanisms by which M13  $\alpha$ CEA promotes antitumor effects, we analyzed if bacteriophage administration induced the infiltration of innate immune cells, such as neutrophils, macrophages and dendritic cells. Palpable CT26-CEA tumors were injected with PBS, M13 WT or M13  $\alpha$ CEA and excised 24 h later to evaluate the presence of macrophages (CD11b<sup>+</sup>, F4/80<sup>+</sup>), neutrophils (CD11b<sup>+</sup>, Ly6G<sup>high</sup>) and dendritic cells (CD11c<sup>+</sup>, MHC-II<sup>+</sup>) by flow cytometry (see contour plot analyses in Fig. 5a). As reported for melanoma [23, 24], intratumoral administration of M13  $\alpha$ CEA bacteriophages promoted the recruitment of both macrophages and neutrophils as

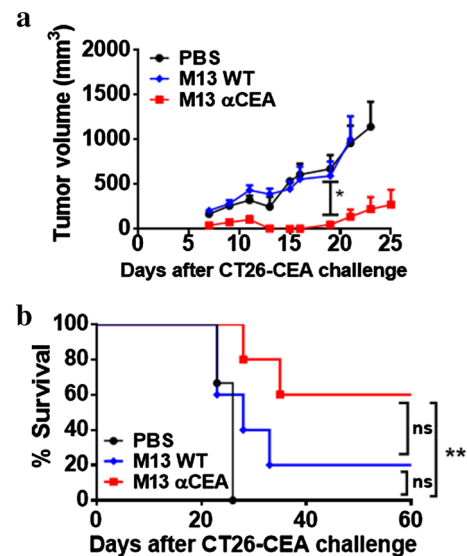


**Fig. 4** Growth of CT26-CEA tumors and survival of mice systemically treated with M13 bacteriophages. BALB/c mice were subcutaneously injected with CT26-CEA tumor cells and 7 days later, mice bearing palpable tumors were intravenously injected with four doses every 2 days of PBS, or  $1 \times 10^{11}$  pfu of either M13 WT or M13  $\alpha$ CEA bacteriophages. Tumor growth (a) and survival curves (b) data from groups treated with PBS (circles), M13 WT (diamonds), M13  $\alpha$ CEA (squares) are shown. Representative data of at least two independent experiments using 5 mice per group are shown. The mean  $\pm$  SEM are shown. Survival curves were analyzed by Log-rank (Mantel–Cox) test. \* $p < 0.05$ ; \*\* $p < 0.005$

compared to control treatments (Fig. 5a). Administration of M13  $\alpha$ CEA increased macrophages from  $\sim 24$  to  $\sim 54\%$  of live CD45<sup>+</sup> population, whereas neutrophils increased from  $\sim 6$  to  $\sim 42\%$ . The percentage of tumor-infiltrating dendritic cells seemed to get reduced after M13  $\alpha$ CEA administration from  $\sim 6$  to  $\sim 2\%$ , but this relative reduction was probably due to the great increase in macrophages (twofold) and especially in neutrophils (sevenfold), which outcompete the proportion of dendritic cells. To further study the effect of M13  $\alpha$ CEA administration on dendritic cells, we analyzed their maturation status in tumor-draining lymph nodes, contralateral non-draining lymph nodes and spleen. The frequencies of dendritic cells were not significantly affected in lymphoid organs, although a trend to increase in tumor-draining lymph nodes was observed (data not shown). Interestingly, M13  $\alpha$ CEA bacteriophage administration promoted the upregulation of costimulatory molecules CD80 and CD86 in dendritic cells present at tumor-draining lymph nodes, but not in contralateral lymph nodes (Fig. 5b). Also, levels of CD80 and CD86 were slightly but significantly increased in dendritic cells present in spleen. Altogether these results indicate that M13  $\alpha$ CEA bacteriophage administration promotes tumor infiltration of innate immune cells and maturation of dendritic cells at secondary lymphoid organs.

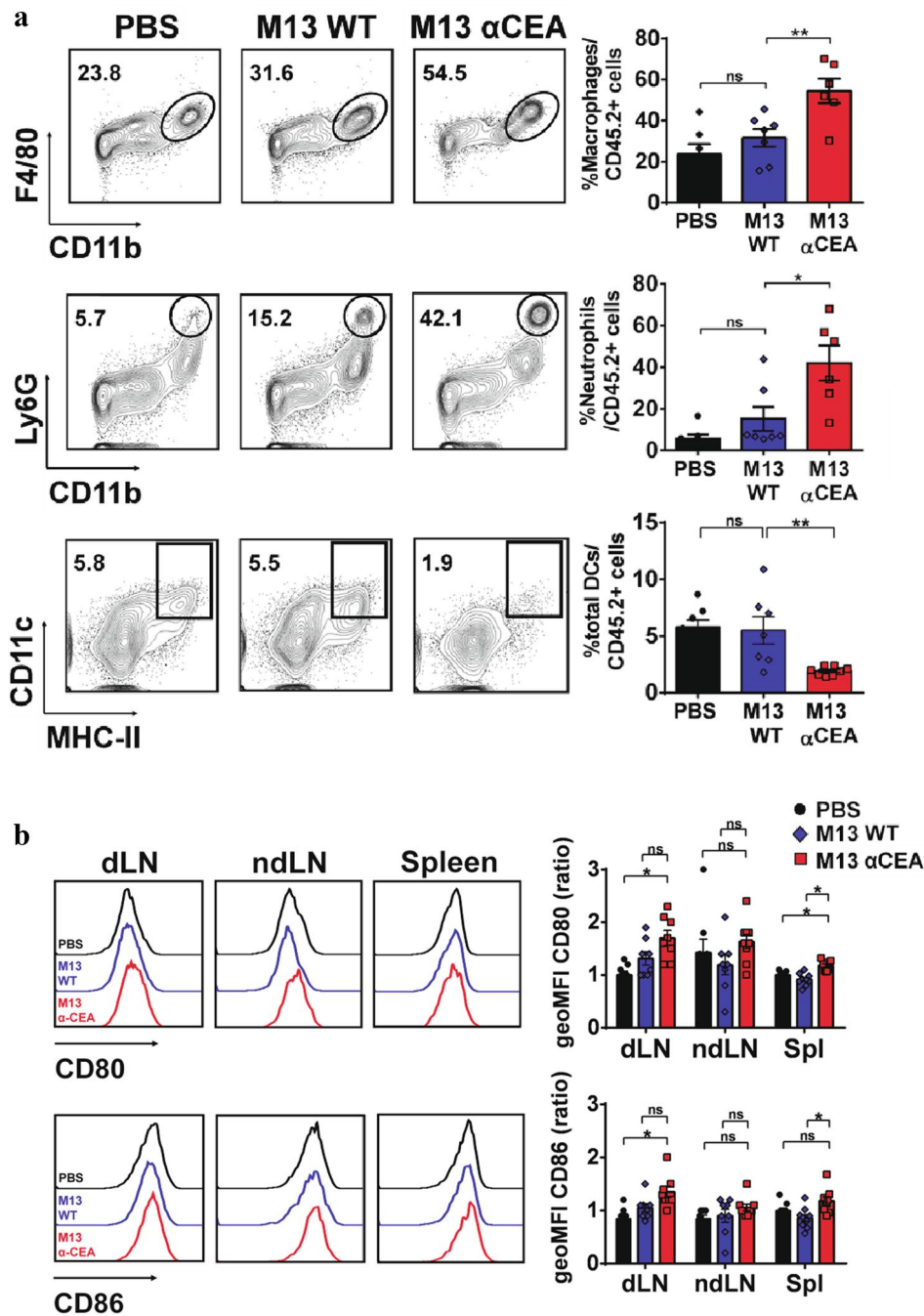


**Fig. 5** Modulation of tumor microenvironment mediated by  $\alpha$ CEA M13 bacteriophages. BALB/c mice were subcutaneously injected with CT26-CEA tumor cells and 7 days later, mice bearing palpable tumors were intratumorally injected with one dose of PBS (circles), or  $1 \times 10^{11}$  pfu of either M13 WT (diamonds) or M13  $\alpha$ CEA (squares) bacteriophages. Twenty-four hours later, mice were killed, and tumors, spleens and draining and non-draining lymph nodes were collected and analyzed by flow cytometry. **a** Representative contour plots analyzing tumor-infiltrating F4/80+CD11b+ macrophages (upper panels), CD11b+Ly6G<sup>high</sup> neutrophils (middle panels) and CD11c+MHC-II+ dendritic cells (DCs) (lower panels) indicating the percentage of each population within the respective region (ellipse,

circle or rectangle, respectively) for each treatment group and the quantification including different animals (right panels). **b** Representative histograms (left panels) and quantification of geometric mean fluorescence intensity (geoMFI, right panels) of surface expression of costimulatory molecules CD80 (upper panels) and CD86 (lower panels) on CD11c+MHC-II+DCs at secondary lymphoid organs, including tumor-draining lymph nodes (dLN), contralateral non-draining lymph nodes (ndLN) and spleen (Spl) for the different treatment groups. Data are representative of at least two independent experiments using 7–9 mice per group. Data correspond to mean  $\pm$  SEM. \* $p < 0.05$ ; \*\* $p < 0.005$ ; ns non-significant



## The antitumor effect of M13 $\alpha$ CEA bacteriophages is mediated by cytotoxic CD8 T cells

Given that cytotoxic CD8 T cells are major effectors of antitumor immune responses, we aimed to evaluate the contribution of these cells to the antitumor effect mediated by M13  $\alpha$ CEA bacteriophage administration. To this end, tumor challenge experiments with CT26-CEA cells were performed in mice that were depleted of CD8 T cells by i.p. injection of anti-CD8 antibody prior and during bacteriophage administration. As control treatment, mice were injected with an isotype-matched antibody. Similar to results shown in Fig. 2, M13  $\alpha$ CEA bacteriophage administration significantly suppressed the growth of CT26-CEA tumors and extended survival of mice treated with control antibody (Fig. 6a). Remarkably, tumor suppression and extended survival were completely abrogated in mice depleted from CD8 T cells (Fig. 6b), which indicates that M13  $\alpha$ CEA bacteriophage-mediated protection relies on the antitumor activity of cytotoxic CD8 T cells. Finally, to test whether a M13 bacteriophage-mediated tumor rejection would lead to systemic adaptive immune responses against tumor-derived antigens, mice that survived to CT26-CEA challenge were re-challenged with the same cells in the opposite flank. A group of naïve mice were included as controls. Interestingly, these mice were completely protected from re-challenge regardless of whether they had received WT or  $\alpha$ CEA

bacteriophages (Fig. 6c). These results indicate that M13 bacteriophage-mediated tumor rejection induces adaptive immune responses against tumor-derived antigens and that scFv-mediated CEA-targeting is important to potentiate the antitumor effects induced by M13 bacteriophages.

## Discussion

More effective therapies are needed to improve the treatment of CRC patients, especially at advanced stages of the disease. The immune system has the potential to fight cancer mainly through cytotoxic CD8 T cells, which efficiently recognize and destroy tumor cells. However, clinically relevant tumors actively generate an immunosuppressive microenvironment that inhibits antitumor immune responses and renders CD8 T cells dysfunctional or hyporesponsive [12–16]. Therefore, overcoming tumor-induced immunosuppressive microenvironment is crucial to achieve protective antitumor immune responses. Based on its ability to activate innate immune cells and promote a pro-inflammatory milieu, we engineered a M13 bacteriophage to display a CEA-specific scFv and bind to the surface of CEA-expressing tumor cells. Moreover, CEA-specific scFv molecules have the potential to inhibit the different malignant functions that have been described for CEA [29–35]. Both intratumoral and systemic administration of  $\alpha$ CEA M13 bacteriophages suppressed

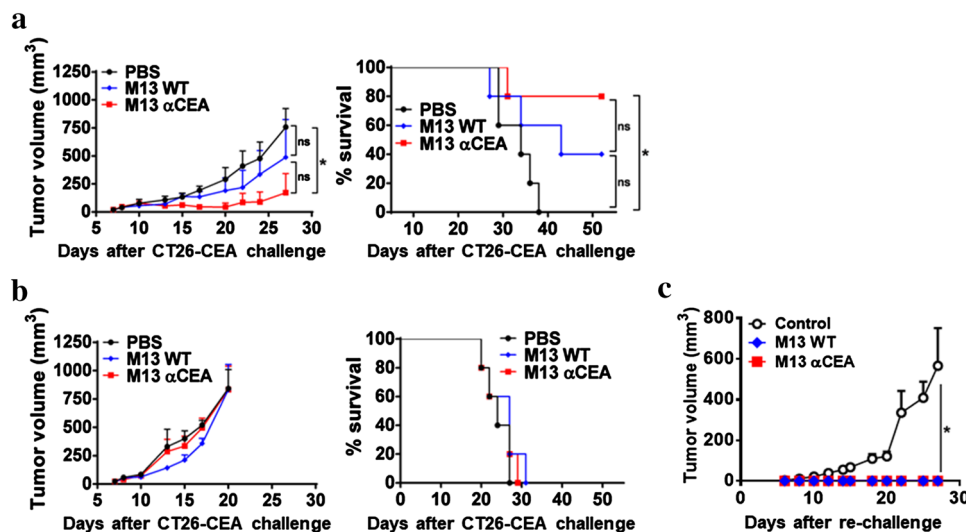


**Fig. 6** Dependence on CD8<sup>+</sup> T cells and long-term protection of mice treated with M13 bacteriophages. C57BL/6 mice were subcutaneously injected with CT26-CEA tumor cells (day 0) and intraperitoneally injected with 0.01 mg of control isotype (a) or anti-CD8 depleting (b) antibodies on days 1, 2, 3, 7, 10 and 13 after tumor challenge. Seven days after tumor challenge, mice bearing palpable tumors were intratumorally injected with four doses every 2 days (days 7, 9, 11 and 13) of PBS, or  $1 \times 10^{11}$  pfu of either M13 WT or M13  $\alpha$ CEA bacteriophages. Tumor growth (left panels) and survival

curves (right panels) for groups treated with PBS (circles), M13 WT (diamonds), M13  $\alpha$ CEA (squares) are shown. c Mice treated with M13 WT and M13  $\alpha$ CEA that survived to CT26-CEA challenge were injected 60 days later with CT26-CEA cells in the opposite flank and tumor growth was registered. Naïve mice (circles) were used as controls. Representative data of at least two independent experiments using 5–6 mice per treatment group are shown. The mean  $\pm$  SEM are shown. Survival curves were analyzed by Log-rank (Mantel–Cox) test. \* $p < 0.05$ ; ns non-significant

tumor growth and extended survival in mouse models of colorectal cancer, involving a CD8 T-cell-dependent mechanism. Although WT M13 showed a moderate antitumor effect, scFv-mediated targeting of M13 bacteriophages to CEA was shown to achieve more robust protection. Clearance of unspecific WT M13 bacteriophages from the tumor must occur fast, while specific M13  $\alpha$ CEA bacteriophages can be retained for longer periods of time by interacting with CEA at the surface of tumor cells, prolonging the time for recognition. Hence, scFv fragments against CEA are essential to maintain M13 bacteriophages associated at the cell surface of tumor cells to potentiate innate immune activation within the tumor microenvironment. In addition, it is possible that targeting CEA by scFv molecules contained in the bacteriophage has an important impact on inhibiting the mechanisms by which CEA promotes malignant features of colorectal cancer cells, including cell-to-cell interactions, epithelial-to-mesenchymal transition, invasiveness, angiogenesis, suppression of differentiation and apoptotic signaling, etc., [31–35, 40].

Bacteriophages are considered safe for human health since they have no tropism for eukaryotic cells [41]. In particular, M13 bacteriophage exclusively infects enterobacterium *E. coli* expressing F pilus, propagating without lysing their host, which allows for an easy production and purification [42]. M13 bacteriophages engineered to display scFv fragments is a broadly studied technique used for high-throughput screening of human antibody libraries, also known as phage display technology. In addition, M13 bacteriophage is a highly immunogenic agent because it contains single-stranded DNA that can activate several innate immune receptors present in innate immune cells and can be used to trigger both humoral and cellular immune responses [21, 22]. Therefore, engineered M13 bacteriophages displaying tumor-specific scFv represent a cost-effective platform to develop strategies for cancer immunotherapy aiming to disrupt the tumor-induced immunosuppressive microenvironment, as well as CEA-dependent malignant features of CRC cells.

In accordance with the results obtained by Eriksson and coworkers in a melanoma model [23, 24], we observed that administration of the  $\alpha$ CEA M13 bacteriophage promoted infiltration of neutrophils and macrophages into tumors (Fig. 4). These myeloid cells have been involved in both supporting and suppressing tumor progression [43, 44]. The opposing roles of neutrophils and macrophages in antitumor response are explained by the high plasticity of these cells, which can transit between pro-inflammatory type-1 and pro-tumoral type-2 phenotypes [45, 46]. Tumor-associated macrophages (TAM) and neutrophils (TAN) present in established tumor at the steady state preferentially display a type-2 phenotype that contributes to a chronic inflammation that promotes tumor progression by enhancing cancer cell

proliferation, invasion and metastasis, promoting angiogenesis, remodeling the extracellular matrix, as well as suppressing antitumor immune responses [47, 48]. In contrast, during acute inflammation, induced by, for example, administration of scFv-targeted bacteriophages or TLR agonists, the infiltration neutrophils and macrophages displaying a type-1 pro-inflammatory phenotype has been reported to occur [24]. Type-1 (N1) neutrophils and (M1) macrophages can directly eliminate tumor cells and promote antitumor activity of other cells from the innate and adaptive immune arms, including cytotoxic CD8 T cells [49]. In CRC patients, TAN density has been associated with better prognosis and better response to 5-fluorouracil chemotherapy [50]. In lung cancer patients, it has been demonstrated that activated neutrophils isolated from malignant and nonmalignant lung tissue are able to stimulate T-cell proliferation and IFN- $\gamma$  production. Then in a positive-feedback loop, activated T cells reciprocally induce the upregulation of costimulatory molecules on neutrophils, which further boosted T-cell proliferation. Similarly, M1 macrophages have been shown to promote T-cell activation in the tumor microenvironment and T-cell-derived IFN- $\gamma$  to exacerbate M1 polarization [51]. Moreover, exogenous stimuli, including TLR agonists such as LPS or CpG motif-containing DNA can reprogram these myeloid cells from type-2 to type-1 pro-inflammatory phenotype [52]. These observations are consistent with our results showing that  $\alpha$ CEA M13 bacteriophage administration strongly promotes tumor infiltration of neutrophils and macrophages and provides antitumor protection that was abrogated in the absence of CD8 T cells. Even if our results indicate that direct antitumor effects ascribed to neutrophils and macrophages did not play a major role in mediating the antitumor response (Fig. 6), CD8 T cells may be promoting antitumor activity of neutrophils and macrophages to achieve more robust protection. The treatment with  $\alpha$ CEA M13 bacteriophages generated also an increase in the expression of costimulatory molecules CD80 and CD86 in dendritic cells present in secondary lymphoid organs such as draining lymph nodes and spleen (Fig. 5b), which may indicate that dendritic cells are either activating pre-existing tumor-specific T cells or generating de novo antitumor T-cell responses. Indeed, mice treated with either bacteriophage that survived the initial CT26-CEA challenge, were completely protected against re-challenge performed 60 days later (Fig. 6c). Our work supports the notion of the “danger model” [53], in which the presence of exogenous infectious agents at the tumor site, in this case M13 bacteriophages, can result in tumor regression. It also suggests that the concerted action of innate and adaptive immune cells is required to achieve strong antitumor immune responses. Therefore, CEA-specific M13 bacteriophages represent a potential immunotherapy against CRC.

## Compliance with ethical standards

**Conflict of interest** Nicolas Ferreira and Hans Pieringer are founders of and work for Phage Technologies S.A. All other authors declare that they have no conflict of interest.

**Funding** This work was funded by Grants CONICYT PFB-16 and CONICYT-791100038 (to Alvaro Lladser) from “Comisión Nacional de Investigación Científica y Tecnológica de Chile”; FONDECYT-1171703 (to Alvaro Lladser) and FONDECYT-3130764 (to Paola Murgas) from “Fondo Nacional de Desarrollo Científico y Tecnológico de Chile”; CORFO-INNOVA 12IDL2-13348 (to Alvaro Lladser) from “Corporación de Fomento de la Producción de Chile”.

## References

- Ferlay J, Soerjomataram I, Dikshit R, Eser S, Mathers C, Rebelo M, Parkin DM, Forman D, Bray F (2015) Cancer incidence and mortality worldwide: sources, methods and major patterns in GLOBOCAN 2012. *Int J Cancer* 136(5):E359–E386
- Mandelblatt J, Andrews H, Kao R, Wallace R, Kerner J (1996) The late-stage diagnosis of colorectal cancer: demographic and socioeconomic factors. *Am J Public Health* 86(12):1794–1797
- Benitez-Majano S, Fowler H, Maringe C, Di Girolamo C, Racht B (2016) Deriving stage at diagnosis from multiple population-based sources: colorectal and lung cancer in England. *Br J Cancer* 115(3):391–400
- Iqbal S, Stoehlmacher J, Lenz HJ (2004) Tailored chemotherapy for colorectal cancer: a new approach to therapy. *Cancer Invest* 22(5):762–773
- Stoehlmacher J, Park DJ, Zhang W, Yang D, Groshen S, Zahedy S, Lenz HJ (2004) A multivariate analysis of genomic polymorphisms: prediction of clinical outcome to 5-FU/oxaliplatin combination chemotherapy in refractory colorectal cancer. *Br J Cancer* 91(2):344–354
- Rosenberg SA, Dudley ME (2004) Cancer regression in patients with metastatic melanoma after the transfer of autologous antitumor lymphocytes. *Proc Natl Acad Sci USA* 101(Suppl 2):14639–14645
- Rosenberg SA, Yang JC, Restifo NP (2004) Cancer immunotherapy: moving beyond current vaccines. *Nat Med* 10(9):909–915
- Hamid O, Robert C, Daud A, Hodi FS, Hwu WJ, Kefford R, Wolchok JD, Hersey P, Joseph RW, Weber JS, Dronca R, Gangadhar TC, Patnaik A, Zarour H, Joshua AM, Gergich K, Ellassaiss-Schaap J, Algazi A, Mateus C, Boasberg P, Tumeh PC, Chmielowski B, Ebbinghaus SW, Li XN, Kang SP, Ribas A (2013) Safety and tumor responses with lambrolizumab (anti-PD-1) in melanoma. *N Engl J Med* 369(2):134–144
- Lipson EJ, Sharfman WH, Drake CG, Wollner I, Taube JM, Anders RA, Xu H, Yao S, Pons A, Chen L, Pardoll DM, Brahmer JR, Topalian SL (2013) Durable cancer regression off-treatment and effective reinduction therapy with an anti-PD-1 antibody. *Clin Cancer Res* 19(2):462–468
- Naito Y, Saito K, Shiiba K, Ohuchi A, Saigenji K, Nagura H, Ohtani H (1998) CD8+ T cells infiltrated within cancer cell nests as a prognostic factor in human colorectal cancer. *Cancer Res* 58(16):3491–3494
- Restifo NP, Dudley ME, Rosenberg SA (2012) Adoptive immunotherapy for cancer: harnessing the T cell response. *Nat Rev Immunol* 12(4):269–281
- Fu J, Xu D, Liu Z, Shi M, Zhao P, Fu B, Zhang Z, Yang H, Zhang H, Zhou C, Yao J, Jin L, Wang H, Yang Y, Fu YX, Wang FS (2007) Increased regulatory T cells correlate with CD8 T-cell impairment and poor survival in hepatocellular carcinoma patients. *Gastroenterology* 132(7):2328–2339
- Gajewski TF, Meng Y, Harlin H (2006) Immune suppression in the tumor microenvironment. *J Immunother* 29(3):233–240
- Gajewski TF, Schreiber H, Fu YX (2013) Innate and adaptive immune cells in the tumor microenvironment. *Nat Immunol* 14(10):1014–1022
- Gajewski TF, Woo SR, Zha Y, Spaapen R, Zheng Y, Corrales L, Spranger S (2013) Cancer immunotherapy strategies based on overcoming barriers within the tumor microenvironment. *Curr Opin Immunol* 25(2):268–276
- Gallina G, Dolcetti L, Serafini P, De Santo C, Marigo I, Colombo MP, Basso G, Brombacher F, Borrello I, Zanovello P, Biccato S, Bronte V (2006) Tumors induce a subset of inflammatory monocytes with immunosuppressive activity on CD8+ T cells. *J Clin Invest* 116(10):2777–2790
- Hornung V, Latz E (2010) Intracellular DNA recognition. *Nat Rev Immunol* 10(2):123–130
- Willis AE, Perham RN, Wraith D (1993) Immunological properties of foreign peptides in multiple display on a filamentous bacteriophage. *Gene* 128(1):79–83
- Clark JR, March JB (2006) Bacteriophages and biotechnology: vaccines, gene therapy and antibacterials. *Trends Biotechnol* 24(5):212–218
- De Berardinis P, Sartorius R, Fanutti C, Perham RN, Del Pozzo G, Guardiola J (2000) Phage display of peptide epitopes from HIV-1 elicits strong cytolytic responses. *Nat Biotechnol* 18(8):873–876
- Sartorius R, D’Apice L, Trovato M, Cuccaro F, Costa V, De Leo MG, Marzullo VM, Biondo C, D’Auria S, De Matteis MA, Ciccodicola A, De Berardinis P (2015) Antigen delivery by filamentous bacteriophage fd displaying an anti-DEC-205 single-chain variable fragment confers adjuvanticity by triggering a TLR9-mediated immune response. *EMBO Mol Med* 7(7):973–988
- Hashiguchi S, Yamaguchi Y, Takeuchi O, Akira S, Sugimura K (2010) Immunological basis of M13 phage vaccine: regulation under MyD88 and TLR9 signaling. *Biochem Biophys Res Commun* 402(1):19–22
- Eriksson F, Culp WD, Massey R, Egevad L, Garland D, Persson MA, Pisa P (2007) Tumor specific phage particles promote tumor regression in a mouse melanoma model. *Cancer Immunol Immunother* 56(5):677–687
- Eriksson F, Tsagozis P, Lundberg K, Parsa R, Mangsbo SM, Persson MA, Harris RA, Pisa P (2009) Tumor-specific bacteriophages induce tumor destruction through activation of tumor-associated macrophages. *J Immunol* 182(5):3105–3111
- Shukla GS, Krag DN, Peletskaya EN, Pero SC, Sun YJ, Carman CL, McCahill LE, Roland TA (2013) Intravenous infusion of phage-displayed antibody library in human cancer patients: enrichment and cancer-specificity of tumor-homing phage-antibodies. *Cancer Immunol Immunother* 62(8):1397–1410
- Ishida H, Miwa H, Tatsuta M, Masutani S, Imamura H, Shimizu J, Ezumi K, Kato H, Kawasaki T, Furukawa H, Kawakami H (2004) Ki-67 and CEA expression as prognostic markers in Dukes’ C colorectal cancer. *Cancer Lett* 207(1):109–115
- Hammarstrom S (1999) The carcinoembryonic antigen (CEA) family: structures, suggested functions and expression in normal and malignant tissues. *Semin Cancer Biol* 9(2):67–81
- Hammarström S (1999) The carcinoembryonic antigen (CEA) family: structures, suggested functions and expression in normal and malignant tissues. *Semin Cancer Biol* 9:67–81
- Benchimol S, Fuks A, Jothy S, Beauchemin N, Shirota K, Stanners CP (1989) Carcinoembryonic antigen, a human tumor marker, functions as an intercellular adhesion molecule. *Cell* 57:327–334
- Beauchemin N, Arabzadeh A (2013) Carcinoembryonic antigen-related cell adhesion molecules (CEACAMs) in cancer progression and metastasis. *Cancer Metastasis Rev* 32:643–671

31. Bajenova O, Chaika N, Tolkunova E, Davydov-Sinitsyn A, Gapon S, Thomas P, O'Brien S (2014) Carcinoembryonic antigen promotes colorectal cancer progression by targeting adherens junction complexes. *Exp Cell Res* 324:115–123
32. Bajenova O, Gorbunova A, Evsyukov I, Rayko M, Gapon S, Bozhokina E, Shishkin A, O'Brien SJ (2016) The genome-wide analysis of carcinoembryonic antigen signaling by colorectal cancer cells using RNA sequencing. *PLoS ONE* 11:e0161256
33. Chan CHF, Camacho-Leal P, Stanners CP (2007) Colorectal hyperplasia and dysplasia due to human carcinoembryonic antigen (CEA) family member expression in transgenic mice. *PLoS ONE* 2(12):e1353
34. Ordoñez C, Ra Screaton, Ilantzis C, Stanners CP (2000) Human carcinoembryonic antigen functions as a general inhibitor of anoikis. *Can Res* 60:3419–3424
35. Taheri M, Saragovi HU, Stanners CP (2003) The adhesion and differentiation-inhibitory activities of the immunoglobulin superfamily member, carcinoembryonic antigen, can be independently blocked. *J Biol Chem* 278:14632–14639
36. Cheever MA, Allison JP, Ferris AS, Finn OJ, Hastings BM, Hecht TT, Mellman I, Prindiville SA, Viner JL, Weiner LM, Matrisian LM (2009) The prioritization of cancer antigens: a national cancer institute pilot project for the acceleration of translational research. *Clin Cancer Res* 15(17):5323–5337
37. Rondot S, Koch J, Breitling F, Dubel S (2001) A helper phage to improve single-chain antibody presentation in phage display. *Nat Biotechnol* 19(1):75–78
38. Yamamoto KR, Alberts BM, Benzinger R, Lawhorne L, Treiber G (1970) Rapid bacteriophage sedimentation in the presence of polyethylene glycol and its application to large-scale virus purification. *Virology* 40(3):734–744
39. Aida Y, Pabst MJ (1990) Removal of endotoxin from protein solutions by phase separation using Triton X-114. *J Immunol Methods* 132(2):191–195
40. Bramswig KH, Poettler M, Unseld M, Wrba F, Uhrin P, Zimmermann W, Zielinski CC, Prager GW (2013) Soluble carcinoembryonic antigen activates endothelial cells and tumor angiogenesis. *Can Res* 73:6584–6596
41. Smith LL, Buckley R, Lugar P (2014) Diagnostic immunization with bacteriophage PhiX 174 in patients with common variable immunodeficiency/hypogammaglobulinemia. *Front Immunol* 5:410
42. Marvin DA (1998) Filamentous phage structure, infection and assembly. *Curr Opin Struct Biol* 8(2):150–158
43. Galdiero MR, Bonavita E, Barajon I, Garlanda C, Mantovani A, Jaillon S (2013) Tumor associated macrophages and neutrophils in cancer. *Immunobiology* 218(11):1402–1410
44. Galdiero MR, Garlanda C, Jaillon S, Marone G, Mantovani A (2013) Tumor associated macrophages and neutrophils in tumor progression. *J Cell Physiol* 228(7):1404–1412
45. Fridlender ZG, Sun J, Kim S, Kapoor V, Cheng G, Ling L, Worthen GS, Albelda SM (2009) Polarization of tumor-associated neutrophil phenotype by TGF-beta: "N1" versus "N2" TAN. *Cancer Cell* 16(3):183–194
46. Qian BZ, Pollard JW (2010) Macrophage diversity enhances tumor progression and metastasis. *Cell* 141(1):39–51
47. Mantovani A, Sozzani S, Locati M, Allavena P, Sica A (2002) Macrophage polarization: tumor-associated macrophages as a paradigm for polarized M2 mononuclear phagocytes. *Trends Immunol* 23(11):549–555
48. Mantovani A (2009) The yin-yang of tumor-associated neutrophils. *Cancer Cell* 16(3):173–174
49. Eruslanov EB, Bhojnarwala PS, Quatromoni JG, Stephen TL, Ranganathan A, Deshpande C, Akimova T, Vachani A, Litzky L, Hancock WW, Conejo-Garcia JR, Feldman M, Albelda SM, Singhal S (2014) Tumor-associated neutrophils stimulate T cell responses in early-stage human lung cancer. *J Clin Invest* 124(12):5466–5480
50. Galdiero MR, Bianchi P, Grizzi F, Di Caro G, Basso G, Ponzetta A, Bonavita E, Barbagallo M, Tartari S, Polentarutti N, Malesci A, Marone G, Roncalli M, Laghi L, Garlanda C, Mantovani A, Jaillon S (2016) Occurrence and significance of tumor-associated neutrophils in patients with colorectal cancer. *Int J Cancer* 139(2):446–456
51. Sinha P, Clements VK, Miller S, Ostrand-Rosenberg S (2005) Tumor immunity: a balancing act between T cell activation, macrophage activation and tumor-induced immune suppression. *Cancer Immunol Immunother* 54(11):1137–1142
52. Sica A, Larghi P, Mancino A, Rubino L, Porta C, Totaro MG, Rimoldi M, Biswas SK, Allavena P, Mantovani A (2008) Macrophage polarization in tumour progression. *Semin Cancer Biol* 18(5):349–355
53. Fuchs EJ, Matzinger P (1996) Is cancer dangerous to the immune system? *Semin Immunol* 8(5):271–280